

# Modelling and Simulation of an Electric Motor-Generator Set for Internal Combustion Engine Replacement

Sulemana Abdul Razak<sup>1</sup> and Erwin Normanyo<sup>2</sup>

<sup>1</sup>Department of Electrical and Electronic Engineering, Academic City College, Accra, Ghana

<sup>2</sup>Department of Electrical and Electronic Engineering, Faculty of Engineering, University of Mines and Technology, Tarkwa, Ghana

\*Corresponding author: [sulemana.razak@acity.edu.gh](mailto:sulemana.razak@acity.edu.gh)

*Submitted 01 November 2020, Revised 16 March 2021, Accepted 16 April 2021.*

Copyright © 2021 The Authors.

**Abstract:** In this paper, a squirrel cage induction motor was used as the prime mover of a permanent magnet synchronous electric generator to achieve a motor-generator set purposed for internal combustion (IC) engine replacement. The motor-generator set was modelled and subjected to performance analysis. The two mechanically coupled machines were tested at 400 VAC input in a Matlab/Simulink software version R2018a environment. The simulation results gave satisfactory responses in terms of the output characteristics of the individual machines as well as their combination. Output power of motor-generator set reduced by 1.7% in comparison to that of the synchronous electric generator. The motor-generator set however, achieved an output power efficiency of 96% at 1 pu of excitation. The excitation level of generator played a critical role in the performance of the motor-generator set. It was shown that the squirrel cage induction motor-synchronous electric generator set can serve as a replacement of the IC engine in standalone power supply systems.

**Keywords:** Electric generator; Electric motor-generator set; Matlab/Simulink software; Modelling; Simulation.

## 1. INTRODUCTION

Electrical energy is very crucial to the sustenance of life, from industrial and commercial to domestic use. The most common method of generating electricity is by means of electric generators. Essentially, they convert mechanical energy into electrical energy. Diesel electric generators are a major source of backup power due to ease of transportation, installation, removal, and availability. Induction motors occupy a larger share of industrial drives. They have proven to be very efficient with varied range of torque, speed and power. They produce no pollution and can work perfectly independent of environmental conditions. A Synchronous Electric Generator (SEG) basically converts mechanical power from a prime mover into electrical power. In a SEG, DC current is applied to the rotor winding producing a rotor magnetic field. The rotor is then turned by external means using the prime mover to produce a rotating magnetic field, which induces a 3-phase voltage within the stator winding [1, 2].

Works on motor-generator (M-G) sets or replacement of Internal Combustion (IC) engines have been duly reported in the literature in recent times. Authors in [3] modelled and simulated a DC motor-SEG set in a bid to identify its parameters by way of deriving the nonlinear and linearised dynamic models. In [4], researchers modelled and simulated a passivity-based control 200 W Doubly Fed Induction Generator (DFIG) interconnected with an Induction Motor (IM). Satisfactory mechanical speed-torque tracking control of the IM was achieved. Authors in [5] established a Power-Hardware-in-the-Loop testbed capability for an experimental MW-scale motor – generator set to maintain higher level synchronisation during power distribution network disturbances. In [6], Chanda simulated the electric M-G set as a single phase to 3-phase converter supply in an effort to control the speed of the cycloconverter fed 3-phase induction motor from a single-phase supply source. Results of use of the M-G set were compared with those of a single phase to 3-phase ARNO converter. The author in [7] in a thesis, modelled and simulated unit components of a M-G set for application in hybrid electric vehicles. In [8], authors modelled and simulated Third Harmonic Excitation Brushless Synchronous Generator (THEBSG) to achieve excellent dynamic characteristics and automatic voltage adjustment. The THEBSG outperformed the normal synchronous generator for IM and resistive-inductive loads. Setlak and Kowalik [9] modelled and simulated the Permanent Magnet Synchronous Generator (PMSG) meant for power supply to an electric aircraft. In [10], authors by way of numerical and experimental simulations investigated a M-G set comprising a 2 kW IM as a compensator motor and a variable speed diesel generator with rotating stator. Increased efficiency of operation, reduced fuel consumption and Greenhouse Gas (GHG) emission of the diesel engine were achieved by the use of advanced control. Authors in [11] modelled and simulated the 3-phase Squirrel Cage Induction

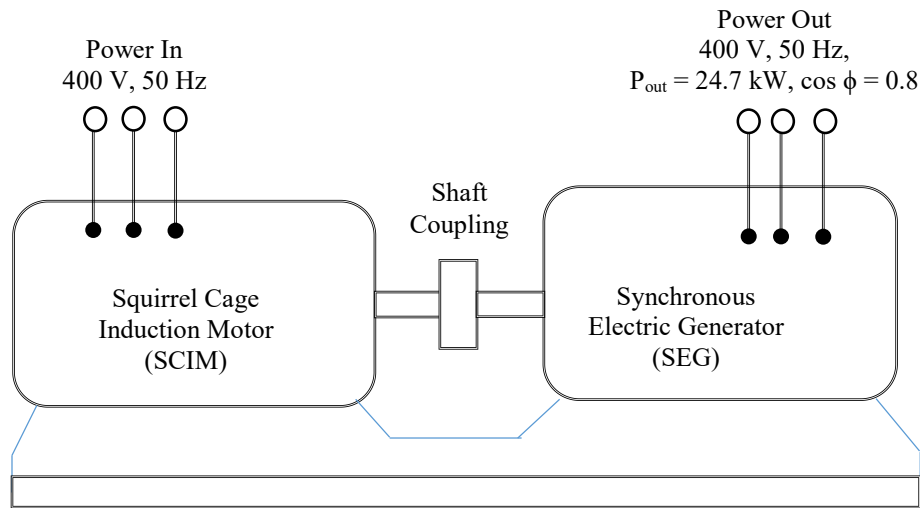


Figure 1. A functional representation of the motor-generator set

Motor (SCIM) for replacement of the IC engine for applications in electric vehicles. Synchronous Reference Frame (SRF) technique was used to simplify the equivalent circuit. The waveforms of induced torque, rotor speed, mechanical output power, efficiency, slip and stator current of the SCIM were generated as outcomes in their simulations.

The related contributions in the literature investigated performance of the M-G set in the domain of parameter identification, variable speed control, power synchronisation and possible applications in electric vehicles and electric aircraft. More importantly, in the works of Salas-Cabrera *et al.* [3], a shunt-excited DC motor was utilized in the M-G set. Also, focus of their paper was on parameter identification of the M-G set and not on replacement of an IC engine by the DC electric motor. Yusof and Mat [11] conducted research on a SCIM that served as replacement of the IC engine in electric vehicle propulsion. This development did not involve the SEG. Electric power production using an M-G set with its input power desirably from possible renewable energy sources such as solar photovoltaic, wind turbines and fuel cells could curtail on GHG emissions and improve power efficiency. A possible green energy powering of the SCIM in the long run assures of IC engine replacement. In this paper, we investigated the M-G set by way of modelling and simulations to ascertain its possible use in replacing the IC engine by examining its output rotational speed and the generated output power. This endeavour is to serve as a prelude to an experimental or field investigation to be geared towards possible use of the SCIM as prime mover of the SEG. The contributions of this paper are firstly, investigation of the M-G set as an option for IC engine replacement and secondly, use of SCIM as prime mover of the SEG. The rest of the paper is organised as follows: In Section 2, the 3-phase SCIM, SEG and the M-G set are modelled and simulated. Simulation results and their discussions are presented in Section 3 and the conclusions are given in Section 4.

## 2. MATHEMATICAL MODELLING AND COMPUTER SIMULATIONS

Mathematical modelling is the description and representation of a system using mathematical concepts and language, mathematical modelling helps to explain a system and to study the effects of different components, and to make predictions about the system's behaviour. Mathematical models are routinely used in the physical and engineering sciences to help understand complex systems and optimise industrial processes [12]. The M-G set is functionally presented in Figure 1.

### 2.1 Modelling of a 3-Phase Induction Motor

An induction motor can be considered as a rotating transformer whose magnetic circuit is separated by an air gap. The stator is considered as primary and rotor is taken as secondary winding. Air gap between the two is considered as the core of the transformer [13]. In deriving the mathematical model of the 3-phase induction motor, it is considered to have a uniform air gap, a squirrel cage type construction and balanced stator and rotor windings, with sinusoidal distributed winding. Its saturation and parameter changes are neglected [14].

#### 2.1.1 Equivalent Circuit of an Induction Motor

The voltage and torque equations that describe the dynamic behaviour of an induction motor are time-varying. It is successfully used to solve such differential equations and it may involve some complexity. A change of variables can be used to reduce the complexity of these equations by eliminating all time-varying inductances, due to electric circuits in relative motion, from the voltage equations of the machine [15].

#### 2.1.2 Equivalent Circuit of an Induction Motor

Dynamic model of the induction motor can be derived based on the quantity of magnetomotive force (MMF) produced in the two-phase and three-phase windings along with equal current magnitudes. Assuming that each of the three-phase windings has  $N_s$  turns per phase and equal current magnitudes, the two-phase winding will have  $3N_s/2$  turns per phase for MMF

equality. The  $d$  and  $q$  axes MMF are found by resolving MMF of the three-phase along  $d$  and  $q$  axes. The common term, the number of turns is cancelled on both sides of equations leaving behind the current equalities. The three-phase stator voltages of an induction machine under balanced conditions can be expressed as in Equations (1), (2) and (3) [16].

$$V_a = \sqrt{2}V_{rms} \sin(\omega t) \quad (1)$$

$$V_b = \sqrt{2}V_{rms} \sin\left(\omega t - \frac{2\pi}{3}\right) \quad (2)$$

$$V_c = \sqrt{2}V_{rms} \sin\left(\omega t + \frac{2\pi}{3}\right) \quad (3)$$

Having  $V_a, V_b$  and  $V_c$  as the line voltages, the relationship between  $\alpha\beta$  of  $abc$  axes is as follows:

$$\begin{bmatrix} V_\alpha \\ V_\beta \end{bmatrix} = \frac{2}{3} \begin{bmatrix} 1 & \frac{1}{2} & -\frac{1}{2} \\ 0 & \frac{\sqrt{3}}{2} & -\frac{\sqrt{3}}{2} \end{bmatrix} \begin{bmatrix} V_a \\ V_b \\ V_c \end{bmatrix} \quad (4)$$

Then the direct ( $V_d$ ) and quadrature ( $V_q$ ) voltages are given in Equation (5).

$$\begin{bmatrix} V_d \\ V_q \end{bmatrix} = \begin{bmatrix} \cos \theta & \sin \theta \\ -\sin \theta & \cos \theta \end{bmatrix} \begin{bmatrix} V_\alpha \\ V_\beta \end{bmatrix} \quad (5)$$

Hence, the instantaneous stator currents of the three-phase system are found using the transformation in Equation (6) while the instantaneous rotor currents are found by the transformation in Equation (7) [14, 17].

$$\begin{bmatrix} i_\alpha \\ i_\beta \end{bmatrix} = \begin{bmatrix} \cos \theta & -\sin \theta \\ \sin \theta & \cos \theta \end{bmatrix} \begin{bmatrix} i_d \\ i_q \end{bmatrix} \quad (6)$$

$$\begin{bmatrix} i_a \\ i_b \\ i_c \end{bmatrix} = \frac{2}{3} \begin{bmatrix} 1 & 0 \\ -\frac{1}{2} & -\frac{\sqrt{3}}{2} \\ \frac{1}{2} & -\frac{\sqrt{3}}{2} \end{bmatrix} \begin{bmatrix} i_\alpha \\ i_\beta \end{bmatrix} \quad (7)$$

where  $i_a, i_b$  and  $i_c$  are rotor currents in phases  $a, b$  and  $c$ , respectively.

### 2.1.3 Flux linkage Equations of Induction Motor

The dynamic model of induction motor in arbitrary reference frame can be represented by using flux linkages as variables. In addition, the flux linkages representation is used in motor drives to highlight the process of decoupling of the flux and torque channels in the induction and synchronous machines. The various flux linkage equations are expressed in Equation (8) to Equation (13) [18].

$$\frac{d\psi_{qs}}{dt} = \omega_b \left[ V_{qs} - \left(\frac{\omega_e}{\omega_b}\right) \psi_{ds} - \left(\frac{R_s}{X_{ls}}\right) (\psi_{mq} - \psi_{qs}) \right] \quad (8)$$

$$\frac{d\psi_{ds}}{dt} = \omega_b \left[ V_{ds} - \left(\frac{\omega_e}{\omega_b}\right) \psi_{qs} - \left(\frac{R_s}{X_{ls}}\right) (\psi_{md} - \psi_{ds}) \right] \quad (9)$$

$$\frac{d\psi_{qr}}{dt} = \omega_b \left[ V_{qr} - \left(\frac{\omega_e - \omega_r}{\omega_b}\right) \psi_{dr} - \left(\frac{R_r}{X_{lr}}\right) (\psi_{mq} - \psi_{qr}) \right] \quad (10)$$

$$\frac{d\psi_{dr}}{dt} = \omega_b \left[ V_{dr} - \left(\frac{\omega_e - \omega_r}{\omega_b}\right) \psi_{qr} - \left(\frac{R_r}{X_{lr}}\right) (\psi_{md} - \psi_{dr}) \right] \quad (11)$$

where

$$\psi_{mq} = X_{ml} \left[ \frac{\psi_{qs}}{X_{ls}} + \frac{\psi_{qr}}{X_{lr}} \right] \quad (12)$$

$$\psi_{md} = X_{ml} \left[ \frac{\psi_{ds}}{X_{ls}} + \frac{\psi_{dr}}{X_{lr}} \right] \quad (13)$$

and

$p$	: number of poles of machine	$\psi_{dr}$	: $d$ -axis rotor magnetising flux,
$d$	: direct axis	$\psi_{ds}$	: $d$ -axis stator magnetising flux
$q$	: quadrature axis	$\psi_{qs}$	: $q$ -axis stator magnetising flux
$s$	: stator variable	$\psi_{qr}$	: $q$ -axis rotor magnetising flux
$r$	: rotor variable	$R_r$	: rotor resistance
$v_{qs}$	: $q$ axis stator voltages	$R_s$	: stator resistance
$v_{ds}$	: $d$ -axis stator voltages	$X_{ls}$	: stator leakage reactance
$v_{qr}$	: $q$ -axis rotor voltages	$X_{lr}$	: rotor leakage reactance
$v_{dr}$	: $d$ -axis rotor voltages	$\omega_e$	: stator angular electrical frequency
$\psi_{mq}$	: $q$ - axis magnetising flux linkages	$\omega_r$	: angular rotor speed
$\psi_{md}$	: $d$ -axis magnetising flux linkages	$\omega_b$	: motor angular electrical frequency

In this paper, the subscripts  $d$  and  $q$  represent the variables in  $d$ - and  $q$ -axes respectively. Respective currents are found by substituting the values of the flux linkages into Equation (14) [13].

$$i_{qs} = \frac{1}{X_{ls}}\psi_{qs} - \psi_{mq}X_{ml} = \left[ \frac{1}{X_m} + \frac{1}{X_{ls}} + \frac{1}{X_{lr}} \right]^{-1} \quad (14)$$

therefore,

$$i_{qr} = \frac{1}{X_{lr}}(\psi_{qr} - \psi_{mq}) \quad (15)$$

$$i_{ds} = \frac{1}{X_{ls}}(\psi_{ds} - \psi_{md}) \quad (16)$$

$$i_{dr} = \frac{1}{X_{lr}}(\psi_{dr} - \psi_{md}) \quad (17)$$

where  $i_{qs}$  and  $i_{ds}$  are stator currents,  $i_{qr}$  and  $i_{dr}$  are rotor currents. Based on the Equations (6)-(14), the electromagnetic torque and rotor speed can be determined as presented in Equations (18) and (19), respectively [19], where  $J$  is moment of inertia,  $T_e$  is electrical output torque and  $T_l$  is load torque.

$$T_e = \left(\frac{3}{2}\right) \left(\frac{p}{2}\right) \left(\frac{1}{\omega_b}\right) (\psi_{ds}i_{qs} - \psi_{qs}i_{ds}) \quad (18)$$

$$\omega_b = \int \frac{p}{2J} (T_e - T_l) \quad (19)$$

Specifications of the selected SCIM (Model Number: ASNA 132-4; Reference Number: IEC 60034-1) as presented in Table 1 are used for the modelling. Figure 2 shows a model of the SCIM in Matlab Simulink software.

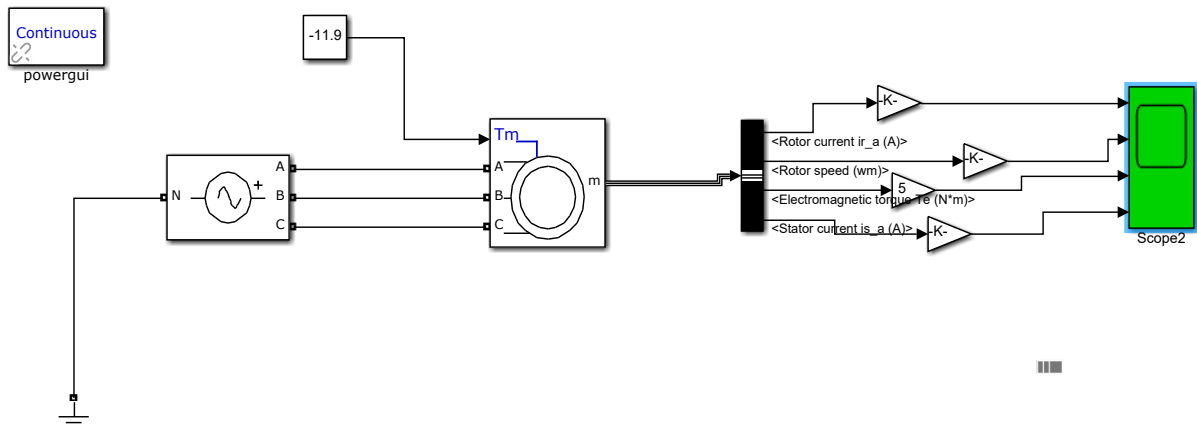
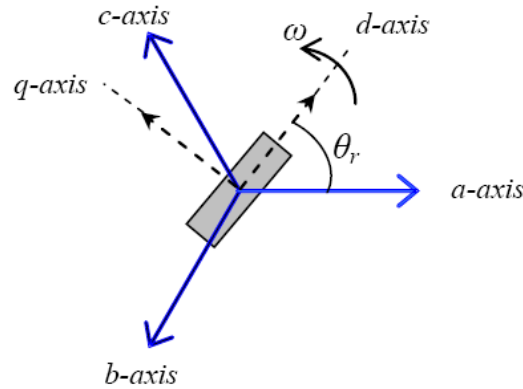


Figure 2. Squirrel cage induction motor model implemented using Matlab-Simulink software

Table 1 Parameters of selected squirrel cage induction motor

Modelling Parameter	Rated Value	Modelling Parameter	Rated Value
Rated power	10 hp, 7.5 kW	Power factor	0.81
Rated stator voltage	400 V	Stator resistance	0.54 ohm
Rated current	15.72 A	Rotor resistance	0.58 ohm
No of poles	4	Stator inductance	88.4 mH
Rated speed	1400/1500 rpm	Rotor inductance	83.3 mH
Frequency	50 Hz	Magnetizing inductance	81.7 mH
Efficiency	85%		

Figure 3. Three phase to  $d$ - $q$  transformation of a permanent magnet synchronous generator

## 2.2 Modelling of the Synchronous Electric Generator

SEG is the fundamental source of energy in modern electrical power networks. It can be modelled with varying levels of complexity. Two different SEG models are widely used, i.e. the sixth order model including leakage reactance, and the fifth order model neglecting leakage reactance [20]. There is a more precise means known as the  $d$ - $q$  model which is aimed at eliminating the dependency of inductances on rotor position. To achieve this, the system of coordinates should be attached to the machine part that has magnetic saliency that is the rotor of SEG [21].

### 2.2.1 $D$ - $q$ Modelling of Synchronous Electric Generator

The  $d$ - $q$  reference frame which is synchronously rotating with the rotor, where  $d$ -axis is aligned with the magnet axis and  $q$ -axis is orthogonal to  $d$ -axis, as shown in Figure 3, is usually used in analysing the synchronous machine. According to Chowdhury [22], Park incorporated a change of variables in the analysis of synchronous machines. The author transformed the stator variables to the rotor reference frame that eliminates the time varying inductances in the voltage equations. Figure 3 shows axes transformation of a permanent magnet synchronous generator (PMSG).

Equation (20) describes the Park transformation used to derive the  $d$ - $q$  model [23]. The inverse transformation yields Equation (21).

$$\begin{bmatrix} f_{ds} \\ f_{qs} \\ f_{os} \end{bmatrix} = \begin{bmatrix} \cos \theta_r & \cos \left( \theta_r - \frac{2\pi}{3} \right) & \cos \left( \theta_r + \frac{2\pi}{3} \right) \\ \sin \theta_r & \sin \left( \theta_r - \frac{2\pi}{3} \right) & \sin \left( \theta_r + \frac{2\pi}{3} \right) \\ \frac{1}{2} & \frac{1}{2} & \frac{1}{2} \end{bmatrix} = \begin{bmatrix} f_{as} \\ f_{bs} \\ f_{cs} \end{bmatrix} \quad (20)$$

$$\begin{bmatrix} f_{as} \\ f_{bs} \\ f_{cs} \end{bmatrix} = \begin{bmatrix} \cos \theta_r & \sin \theta_r & 1 \\ \cos \left( \theta_r - \frac{2\pi}{3} \right) & \sin \left( \theta_r - \frac{2\pi}{3} \right) & 1 \\ \cos \left( \theta_r + \frac{2\pi}{3} \right) & \sin \left( \theta_r + \frac{2\pi}{3} \right) & 1 \end{bmatrix} = \begin{bmatrix} f_{ds} \\ f_{qs} \\ f_{os} \end{bmatrix} \quad (21)$$

where  $\theta_r = \int \omega_r dt$  is angular displacement, and  $f_{as}$ ,  $f_{bs}$  and  $f_{cs}$  are instantaneous quantities which are functions of time, and can be voltages, current, flux linkages or electric charges. The  $q$ -axis and  $d$ -axis voltages in synchronous reference frame are given in Equations (22) and (23), respectively [21].

$$V_q = -i_q R_s - \omega_r \lambda_d + \Delta \lambda_q \quad (22)$$

$$V_d = -i_d R_s - \omega_r \lambda_q + \Delta \lambda_d \tag{23}$$

$V_d$  and  $V_q$  are stator voltages,  $\lambda_d$  and  $\lambda_q$  are stator flux linkages,  $i_d$  and  $i_q$  are stator currents,  $R_s$  is stator resistance and  $\Delta$  is operator  $d/dt$ . If  $\lambda_M$  is the rotor magnetic flux produced, then the stator flux can be written in the form presented in Equation (24) and Equation (25).

$$\lambda_d = -L_d i_d + \lambda_M \tag{24}$$

$$\lambda_q = -L_q i_q \tag{25}$$

Hence,

$$L_d = L_{ls} + L_{md} \tag{26}$$

$$L_q = L_{ls} + L_{mq} \tag{27}$$

$$\lambda_s = \lambda_d + j\lambda_q \tag{28}$$

$$V_s = V_d + jV_q \tag{29}$$

$$i_s = i_d + j i_q \tag{30}$$

The torque equation of the synchronous generator is given by Equation (31) [22].

$$T_g = -\frac{3}{2} p [\lambda_d i_q - \lambda_q i_d] = -\frac{3}{2} p [\lambda_M i_q + (L_d - L_q) i_d i_q] \tag{31}$$

where  $T_g$  is torque developed,  $L_d$  and  $L_q$  are inductances,  $L_{md}$  and  $L_{mq}$  are magnetising inductances and  $L_{ls}$  is stator leakage inductance. The output power efficiency of machine is given by Equation (32) [24].

$$\eta = \frac{60 P_{gen}}{2\pi N T_g} \tag{32}$$

where  $N$  is the speed and  $P_{gen}$  is the power developed. Table 2 gives the modelling parameters of the selected SEG and Figure 4 shows the model of the SEG in Matlab Simulink.

Table 2. Modelling parameters of the selected synchronous electric generator [25]

Modelling Parameter	Symbol	Value	Modelling Parameter	Symbol	Value
Short Circuit Ratio	$R$	0.43	Negative Sequence Reactance ( $\Omega$ )	$X_2$	115
Quadrature Axis Synchronous Reactance ( $\Omega$ )	$X_q$	145	Quadrature Axis Sub Transient Reactance ( $\Omega$ )	$X''_q$	12.4
Direct Axis Synchronous Reactance ( $\Omega$ )	$X_d$	260	Zero Sequence Reactance ( $\Omega$ )	$X_0$	1.5
Direct Axis Transient Reactance ( $\Omega$ )	$X'_d$	22.0	Open Circuit Reactance ( $\Omega$ )	$T'_{do}$	0.66
Direct Axis Sub Transient Reactance ( $\Omega$ )	$X''_d$	10.5	Transient Reactance ( $\Omega$ )	$T'_d$	0.045

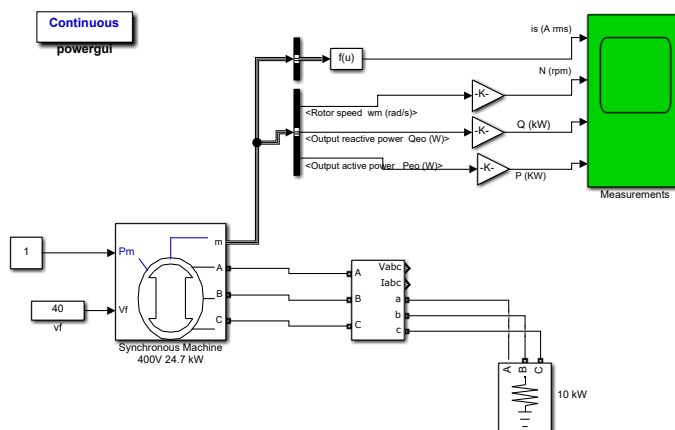


Figure 4. Synchronous electric generator model implemented using Matlab-Simulink software

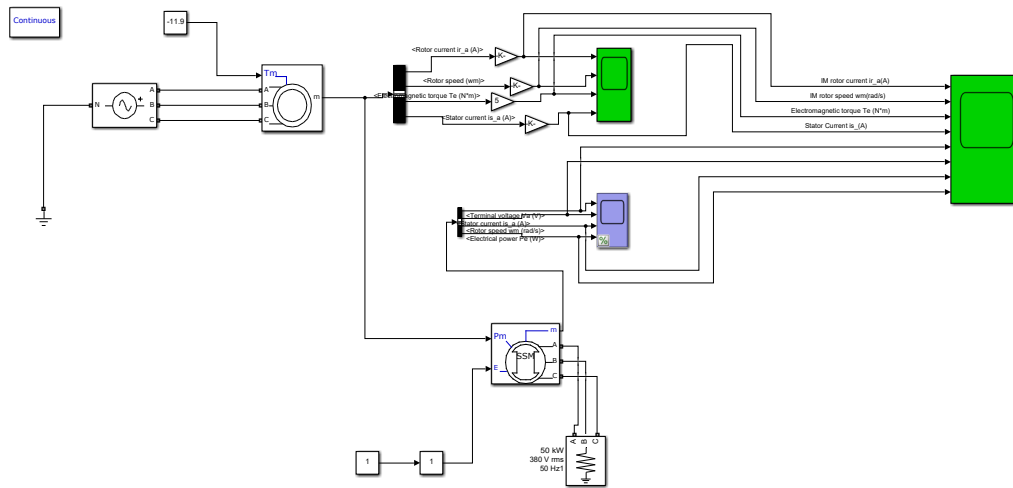


Figure 5. Model of the motor-generator set implemented in Matlab-Simulink software

### 2.3 Modelling of the Motor-Generator Set in Matlab/Simulink

Modelling of the M-G set was conducted by combining the SCIM and the SEG models in Matlab/Simulink page taking cognizance of the stiff coupling between the two machines. Prior to the combining of the two machines, the SCIM model was simulated at 380 V, 1400 rpm and 400 V, 1500 rpm whilst the SEG was simulated at 1 pu and 0.5 pu of field excitation. On the other hand for the SCIM, a focus was given to stator current, rotor speed, electromagnetic torque and the rotor induced current. For the SEG, the signal waveforms of concern were those of the output voltage, speed, output power and stator current. Based on satisfactory validation, the two machines were combined into a SCIM-SEG set. The SCIM-SEG model in Matlab/Simulink is presented in Figure 5.

### 2.4 Computer Simulations

The modelled M-G set system was investigated by way of computer simulations in the Matlab/Simulink software environment. The same considered signal waveforms of the individual machines under the test conditions were monitored for the complete system at rated SCIM input voltage of 400 V for rated speed of 1500 rpm at 1 pu and 0.5 pu of SEG field excitation to ascertain performance of the complete system in terms of rotational speed and output power of the SEG. All variables were monitored with respect to time. Generator excitation level is known to affect its performance.

## 3. RESULTS AND DISCUSSIONS

The simulation results are presented in Figures 6-11. From Figures 6 and 7, both stator and rotor currents oscillated at high frequency at about  $\pm 20$  A for 6.8 secs. The stator current cleared its oscillations whilst the rotor current continued the high frequency oscillations at a reduced amplitude of  $\pm 7$  A for the rest of the 10 secs. For the same 6.8 secs, the rotor speed gradually rose to the required values of 1400 rpm and 1500 rpm, respectively. The electromagnetic torque oscillated at the start of the SCIM for 0.6 secs and gradually rose to a peak of about 36 Nm at 6.6 secs and changed to a reverse peak torque of negative 44 Nm at almost 7 secs. The differences of 20 V and 100 rpm in the stator input voltage and motor speed, respectively hardly made any impact on the results presented in Figures 6 and 7. This development assures of a bit of flexibility in voltage and speed of the SCIM operation.

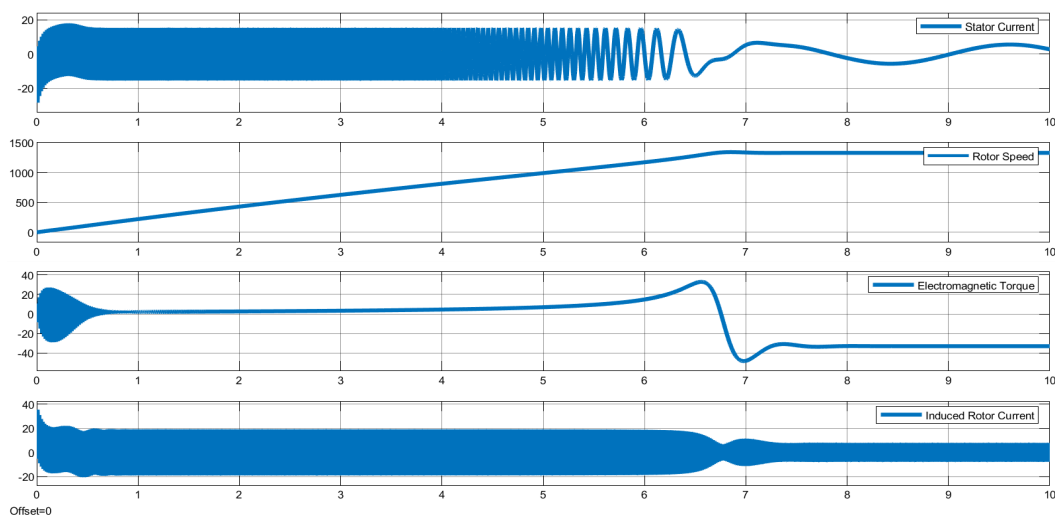


Figure 6. Squirrel cage induction motor at 380 V, 1400 rpm

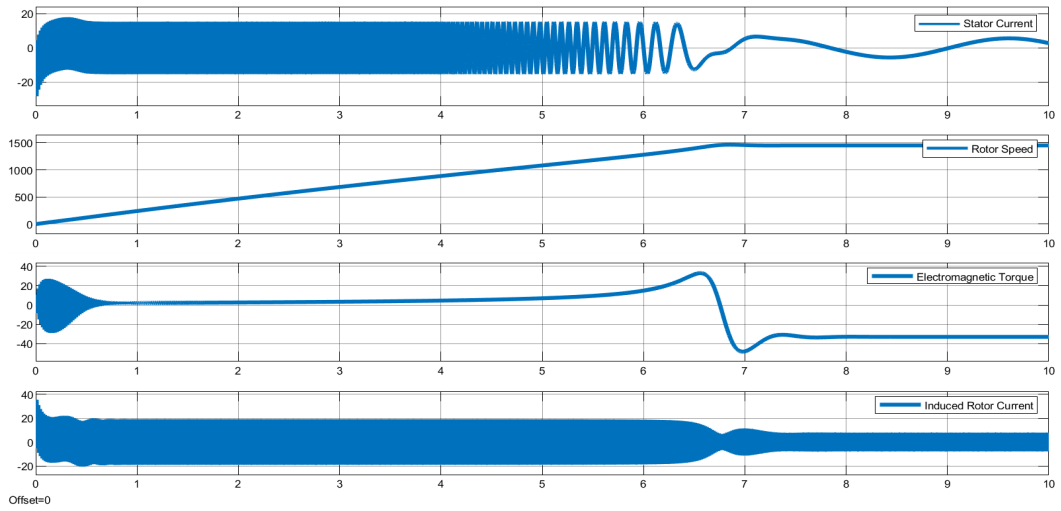


Figure 7. Squirrel cage induction motor at 400 V, 1500 rpm

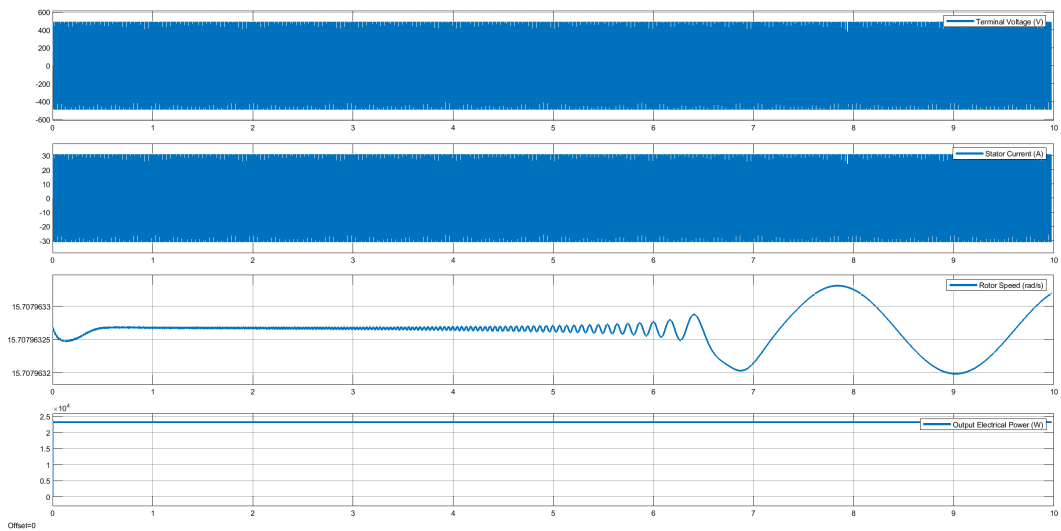


Figure 8. Synchronous electric generator at a field excitation of 1 pu

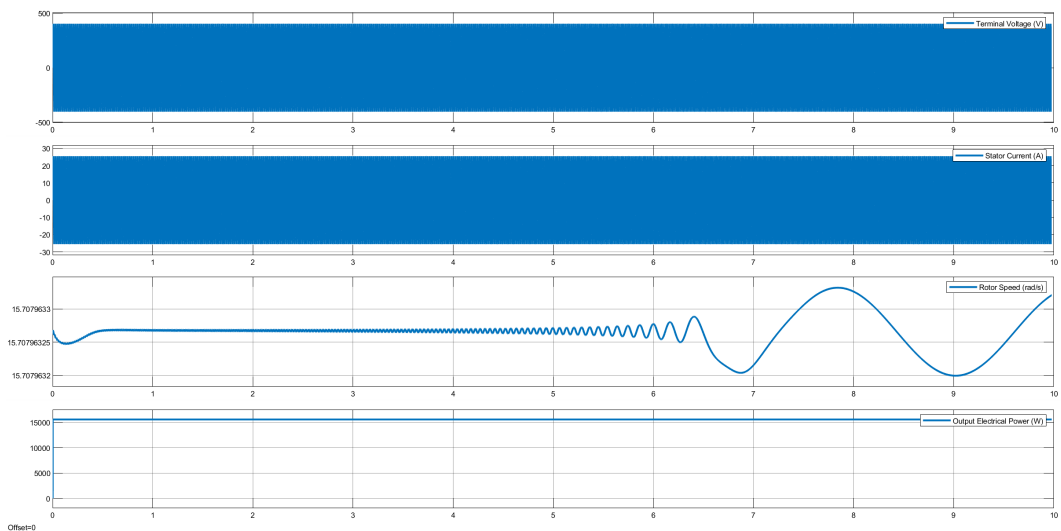


Figure 9. Synchronous electric generator at a field excitation of 0.5 pu

In Figures 8 and 9, the results gave highly desirable sinusoidal waveforms of the SEG terminal voltage and stator current. The rotor speed and output electric power presented constant values with insignificant oscillations, respectively at 1500 rpm (irrespective of field excitation) and 24.4 kW at 1 pu and 15.9 kW at 0.5 pu. At a SEG terminal voltage of 400 V, 0.8 power factor, SCIM input voltage of 400 V and rated speed of 1500 rpm, Figures 10 and 11 show that the M-G set gave a constant

active output power of 23.6 kW at 1 pu and 15.24 kW at 0.5 pu of excitation, respectively. However, for the two values of excitation, the speed of SEG dipped for 0.5 secs and stabilised at 1570 rpm up to 4 secs beyond which it oscillated at diminishing frequencies.

Comparing the M-G set to the SEG in terms of output power, there has been an insignificant 1.7% reduction both at 1 pu and 0.5 pu of generator excitation. However, at an active power rating of 24 kW of SEG, the M-G set achieved a power delivery efficiency of 96.0% at 1 pu and 62% at 0.5 pu of excitation, respectively. A summary of these findings are summarised in Tables 3-6. It stands to reason that the output power and for that matter output power efficiency of the M-G set is highly dependent on the SEG field excitation level.

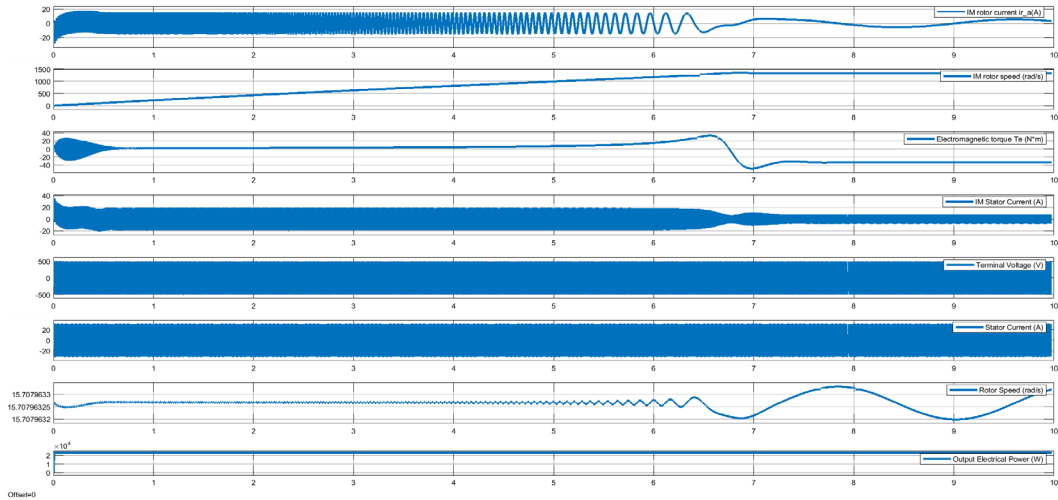


Figure 10. Motor-generator set at 1 pu of SEG field excitation

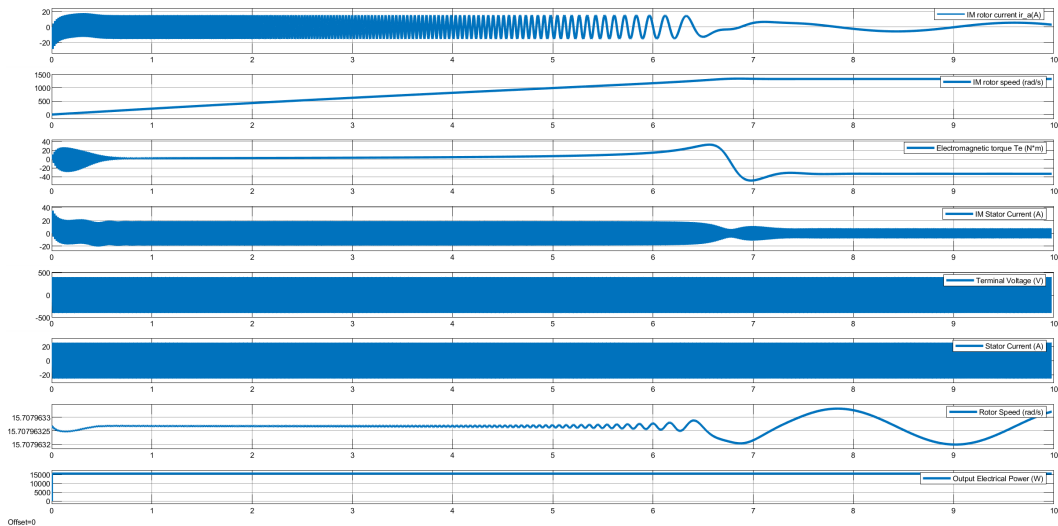


Figure 11. Motor-generator set at 0.5 pu of SEG field excitation

Table 3. SEG test results

Parameter	Max Output Power of SEG (kW)	Output Voltage (V)	Speed of SCIM (rpm)	SEG Stator Current (A)
Output Rating	25	400	1500	15.5
Output Power of SEG at 0.5 pu of field excitation	15.9	400	1500	20
Output Power of SEG at 1 pu of field excitation	24.4	400	1500	25

Table 4. M-G set test results

Parameter	Max Output Power of M-G SET (kW)	Output Voltage (V)	Speed of SCIM (rpm)	SEG Stator Current (A)
Output Rating	25	400	1500	15.5
Output Power of M-G set at 0.5 pu of field excitation	15.5	400	1500	20
Output Power of M-G set at 1 pu of field excitation	24	400	1500	25

Table 5. Output power of SEG and M-G set

Parameter	SEG Output Power (kW)	MG set Output Power (kW)
Output Rating	25	25
Output Power at 0.5 pu of field excitation	15.9	15.5
Output Power at 1 pu of field excitation	24.4	24

Table 6. Output power efficiency of SEG and M-G set at 400 V, 1500 rpm

Parameter	SEG	M-G set	Difference in Efficiency
Output Power Efficiency at 1 pu (%)	97.7	96.0	1.7
Output Power Efficiency at 0.5 pu (%)	63.7	62.0	1.7

#### 4. CONCLUSION

Successful modelling and simulation of an M-G set has been presented in this paper. At a reduction of 1.7% in output power efficiency of the M-G set over the SEG, an output power efficiency of 96.0% at 1 pu of excitation of the M-G set was achieved. The excitation level of generator played a critical role in the performance of the M-G set. In standalone systems, the M-G set is deployable for sustainable electric power generation without the need for an IC engine.

#### REFERENCES

- [1] S. K. Bhattacharya, *Electrical machines*, New Delhi, India: McGraw Hill Education (India) Private Limited, 2014.
- [2] S. Chapman, *Electric machinery fundamentals*, New York, USA: McGraw-Hill Education, 2011.
- [3] R. Salas-Cabrera, O. Martinez-Hernandez, R. Castillo-Ibarra, J. C. Rosas-Caro, A. Gonzalez-Rodriguez, E. N. Salas-Cabrera, H. Cisneros-Villegas, R. Castillo-Gutierrez and G. Hernandez-Palmer, On the modelling and parametric identification of a motor-generator set, *Proceedings of the World Congress on Engineering and Computer Science*, San Francisco, USA, 2010, Vol. II, 1-7.
- [4] M. Becherif, A. Bensadeq, E. Mendes, A. Henni, P. Lefley and M. Y. Ayad, From dynamic modelling to experimentation of induction motor powered by doubly-fed induction generator by passivity-based control, in *Electric Machines and Drives*, Print Edition, M. Chomat, Ed. Shanghai, China: InTech, 2011, 113-144.
- [5] Q. Hong, I. Abdulhadi, A. Roscoe and C. Booth, Application of a MW-scale motor-generator set to establish power-hardware-in-the-loop capability, *Proceedings of the 7th IEEE PES International Innovative Smart Grid Technologies Conference Europe (ISGT-Europe)*, Torino, Italy, 2017, 1-6.
- [6] A. Chanda, Use of Arno converter and motor-generator set to convert a single-phase AC supply to a three-phase AC for controlling the speed of a three-phase induction motor by using a three-phase to three-phase cycloconverter, *International Journal of Electrical Engineering and Technology*, 7(2), 2016, 19-28.
- [7] Y. Narkhede, *Simscape modelling of motor-generator unit components for hybrid electric vehicle*, MSc Thesis, School of Electrical and Computer Engineering, Georgia Institute of Technology, Atlanta, USA, 2016.
- [8] W. Liu and C. Zhu, Modelling and simulation of excitation system for third harmonic brushless synchronous generator, *IOP Conf. Series: Materials Science and Engineering*, 2019, 563, 032038.
- [9] L. Setlak and R. Kowalik, Model and simulation of permanent magnet synchronous machine (PMSM) of the electric power supply system (EPS) in accordance with the concept of a more electric aircraft (MEA), *ITM Web of Conferences*, 2018, 16, 03004, 1-6.
- [10] M. Mobarra, B. Tremblay, M. Rezkallah and A. Ilinca, Advanced control of a compensator motor driving a variable speed diesel generator with rotating stator, *Energies*, 2020, 13, 2224.
- [11] Y. Yusof and K. Mat, Modelling, simulation and analysis of induction motor for electric vehicle application, *International Journal of Engineering & Technology*, 7(3), 2018, 145-150.

- [12] D. M. Ben and O. C. O. Richard, From mathematical models to clinical reality, in: *Principles of Tissue Engineering*, 5th edition, Academic Press/Elsevier, 2020.
- [13] M. Batool and A. Ahmad, Mathematical modelling and speed-torque analysis of three phase squirrel cage induction motor using Matlab Simulink for electrical machines laboratory, *International Electrical Engineering Journal*, 4(1), 2013, 880–889.
- [14] P. L. Ratnani and A. G. Thosar, Mathematical modelling of a 3-phase induction motor using MATLAB/Simulink, *International Journal of Modern Engineering Research*, 4(6), 2014, 201–207.
- [15] M. K. Singh, M. Chauhan, A. K Singhal and N. Saxena, A methodology to develop a simulink model of three phase induction motor, *International Journal of Emerging Technology and Advanced Engineering*, 4(1), 2014, 93–97.
- [16] M. K. Miloje, Equivalent circuit improvement method for induction motor efficiency, *Journal of Electrical Engineering*, 25(1), 2012, 31–42.
- [17] A. W. Leedy, Simulink/Matlab dynamic induction motor model for use as a teaching and research tool, *International Journal of Soft Computing and Engineering*, 3(4), 2013, 102–107.
- [18] S. A. Shah, M. K. Rashid and L. Bhatti, Direct quadrature (d-q) modelling of 3-phase induction motor using Matlab/Simulink, *Canadian Journal on Electrical and Electronics Engineering*, 3(5), 2012, 23–243.
- [19] A. N. B. Alsammak and M. F. Thanoon, An improved transient model of an induction motor including magnetising and leakage inductances saturated effect, *International Journal of Engineering and Innovative Technology*, 3(10), 2014, 5–12.
- [20] M. Sattouf, Simulation model of hydro power plant using Matlab/Simulink, *International Journal of Engineering Research and Applications*, 4(1), 2014, 295–301.
- [21] A. A. Ansari and D. M. Deshpande, Mathematical model of asynchronous machine in MATLAB Simulink, *International Journal of Engineering Science and Technology*, 2(5), 2010, 1260–1267.
- [22] M. M. Chowdhury, *Modelling and control of direct drive variable speed wind turbine with interior permanent magnet synchronous generator*, PhD Thesis, University of Tasmania, Australia, 2014.
- [23] J. McCalley, D-Q transformation of synchronous machines, *Power Point Presentation*, [www.slidserve.com](http://www.slidserve.com), 2014.
- [24] K. Hiroyasu, K. Z. Mehdi and S. Hidetsugu, Efficiency estimation of synchronous generator for marine application and verification with shop trial data and real ship operation data, *IEEE Access*, 8(1), 2020, 195541–195550.
- [25] E. Anbarasu and M. Karthikeyan, Modelling of induction motor and fault analysis, *International Journal of Engineering Science and Innovative Technology*, 2(4), 2013, 383–393.